On-surface reactivity of disubstituted-bianthryl molecules on Cu(111) and Au(111) surfaces

Elie Geagea,[1] Judicael Jeannoutot,[1] Frank Palmino,[1] Frédéric Chérioux[1,z]

[1] Université de Franche-Comté, FEMTO-ST, CNRS, UFC, 25B avenue des Montboucons, 25030 Besancon, France.
[z] Corresponding author: frederic.cherioux@femto-st.fr

Abstract
On-surface π-conjugated 1D polymers, like graphene nanoribbons, have emerged as a class of promising materials. On-surface chemical properties of 9,9'-bianthryl molecules are widely developed as they can be used as starting building blocks to provide graphene nanoribbons. Here, we propose to investigate the chemical behavior of 10,10'-disubstituted-9,9'-bianthryl molecules on Cu(111) and Au(111) surfaces by using scanning tunneling microscopy under ultra-high vacuum. We demonstrated that the balance between molecule-molecule interaction, molecule-substrate interaction, and molecular rearrangement, drastically alter the chemical properties of the adsorbed molecule by thermal annealing.

Introduction
During the three two decades, molecular self-assembly has been widely investigated on different kinds of substrates [1–5]. More recently, on-surface chemistry has emerged to elaborate covalent nanostructures [6–18]. All these nanostructures have been obtained by bottom-up approaches and their structures are atomically precise, as proven by scanning probe microscopies, that can be used for great potential applications in molecular electronics, spintronics, energy, catalysis, and other fields. Graphene nanoribbons (GNRs) are 1D graphene stripes that are widely investigated due to their remarkable electronic properties compared to 2D graphene [19–20]. To achieve GNRs with a well-defined edge configuration and width, and accordingly control these electronic properties, growth from wisely-chosen molecular building-blocks was optimized thanks to atomic-scale characterization using scanning probe microscopies under ultra-high vacuum (UHV) [21–38]. The two most commonly used precursors for the on-surface synthesis of GNRs are 10,10'-dihalogenated-9,9'-bianthryl derivatives [21–29] and 9,9'-bianthryl [30–38]. 10,10'-dihalogenated-9,9'-bianthryl derivatives lead to the formation of a large variety of GNRs on different kinds of coinage metal surfaces in a two-steps reaction: (i) a thermally induced Ullmann cross-coupling followed by (ii) a cyclodehydrogenation [21–29]. Non-halogenated 9,9'-bianthryl derivatives lead to chiral (3,1)-GNRs, but only on a copper surface. [30–38] After few controversies, [36–38] the currently accepted reactional mechanism for the growth of chiral (3,1)-GNRs on a Cu(111) surface is based on a first thermal annealing leading to a protopolymer thanks to on surface-assisted generation of a 2,2'-diradical species. Then, further heating gives the targeted chiral (3,1)-GNR as result of ring-closure driven by a cyclodehydrogenation. Most of the reaction intermediates involved in this mechanism have been observed. [30–38]

Here, we investigate the on-surface chemistry of two 10,10'-disubstituted-9,9'-bianthryl derivatives induced by thermal annealing on Cu(111) and Au(111). Experiments were performed in ultra-high vacuum (UHV) and all adsorbates are fully characterized by scanning tunneling microscopy that provides images with submolecular resolution. We demonstrate that the molecule-surface couple plays a major role in the chemical transformation. In the case of Cu(111), 10,10'-disubstituted-9,9'-bianthryl are not transformed into (3,1)-GNRs due to the lack of reactivity of the starting building blocks, while on Au(111), surface only the formation of coordination polymers is observed.

Experimental

Molecules

All reagents were purchased from Aldrich, except $Pd(PPh_3)_4$ which was purchased from Strem chemical, and used as received. The silica gel used for column chromatography was purchased from Merck. The deuterated NMR solvents were purchased from Euriso-top. The NMR spectra were recorded using a Bruker AC-300 MHz spectrometer. The two molecules, 10,10'-di-(4''-cyanophenyl)-9,9'-bianthryl (CPBA) and 10,10'-di-(4''-pyridyl)-9,9'-bianthryl (PBA) were synthesized by a procedure adapted from the literature [39-40]. Basically, 10,10'-dibromo-9,9'-bianthryl, 4'-cyanophenyl boronic acid pinacol ester or 4'-pyridyl boronic acid pinacol ester, cesium carbonate and $Pd(PPh_3)_4$ as a catalyst were dissolved in tetrahydrofuran. The resulting solid, obtained after removing of volatiles, was purified by column chromatography (silica gel, cyclohexane/dichloromethane 1:1) to give a pure white solid [41].

Surfaces and STM experiments

The first step consists of the preparation of the Cu(111) and Au(111) surfaces by argon ions sputtering cycles at 1.2 kV followed by thermal annealing at 723 K and 673 K for Cu111) and Au(111), respectively. This takes place inside a preparation chamber maintained under UHV conditions with a base pressure lower than $2 \cdot 10^{-10}$ mbar and coupled to an Omicron variable temperature Scanning Tunneling Microscope (Omicron VT-STM XA). Once the cleanness of Cu(111) and Au(111) surface is confirmed by analysis of STM images, we proceed to the deposition of molecules by thermal sublimation from a quartz crucible with a corresponding temperature of 458 K for PBA and 468 K for CPBA. During deposition the substrate was held at room temperature then transferred and cooled to 110 K on the STM stage for acquiring images. Each image process was carried out using SPIP software.

Results

We synthesized 10,10'-di(4''-pyridyl)-9,9'-bianthryl (PBA) and 10,10'-di(4''-cyanophenyl)-9,9'-bianthryl (CPBA) respectively, that are based on bianthryl core surrounded by two lateral aryl groups covalently bound to the 10 and 10' positions (Figure 1). We chose cyanophenyl and pyridyl groups because they promote the formation of supramolecular self-assemblies on different types of surfaces [3-5]. The length is 1.67 nm and 2.08 nm for PBA and CPBA, respectively, while the distance between the extremities of the two anthracenyl rings is 0.79 nm and (Figure 1).

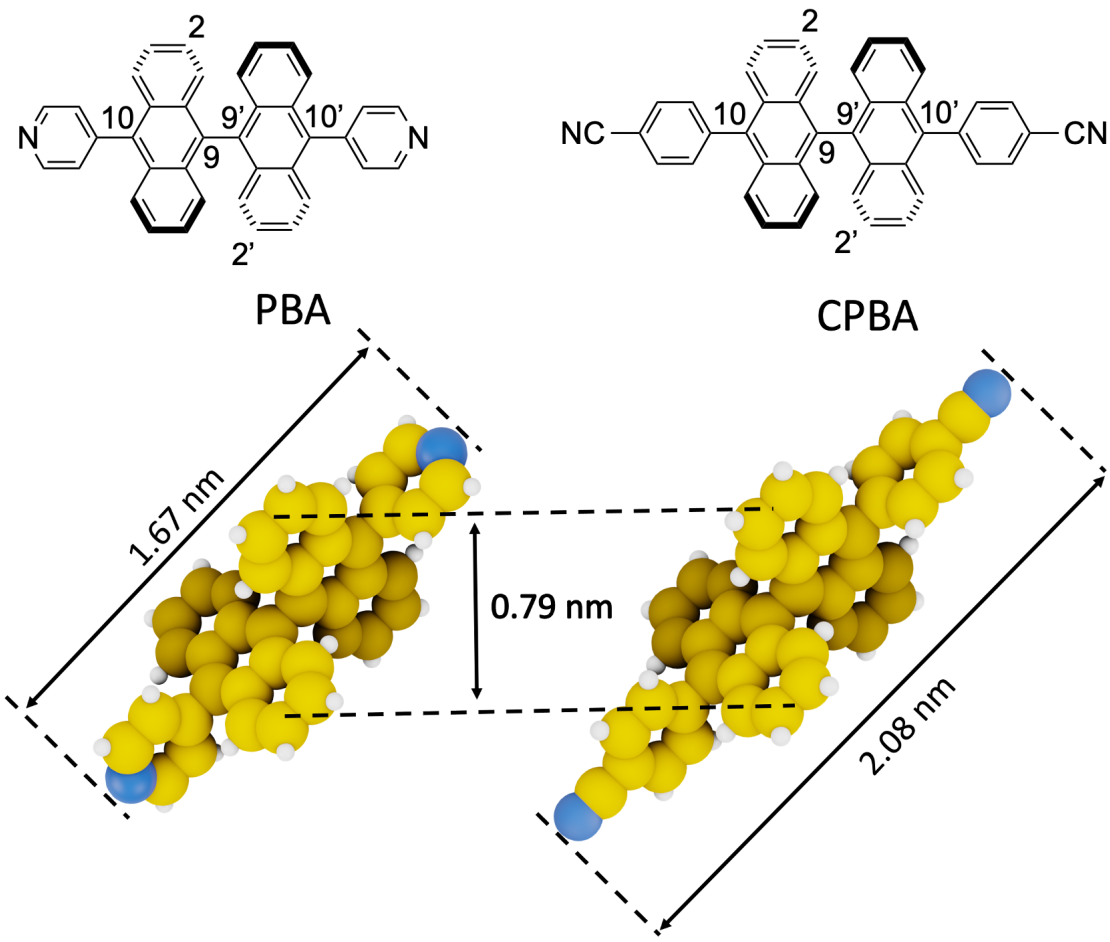

Figure 1. CPK models of 10,10'-di-(4''-pyridyl)-9,9'-bianthryl (PBA) and 10,10'-di-(4''-cyanophenyl)-9,9'-bianthryl (CPBA) molecules respectively.

PBA and CPBA molecules were deposited at the monolayer threshold by thermal sublimation under UHV on a Cu(111) and an Au(111) substrate kept at room temperature. As revealed in STM images recorded at 110 K, no isolated molecule was observed but only large extended 2D islands on the two chosen surfaces, each building-up of highly organized periodic protrusions (Figure 2).

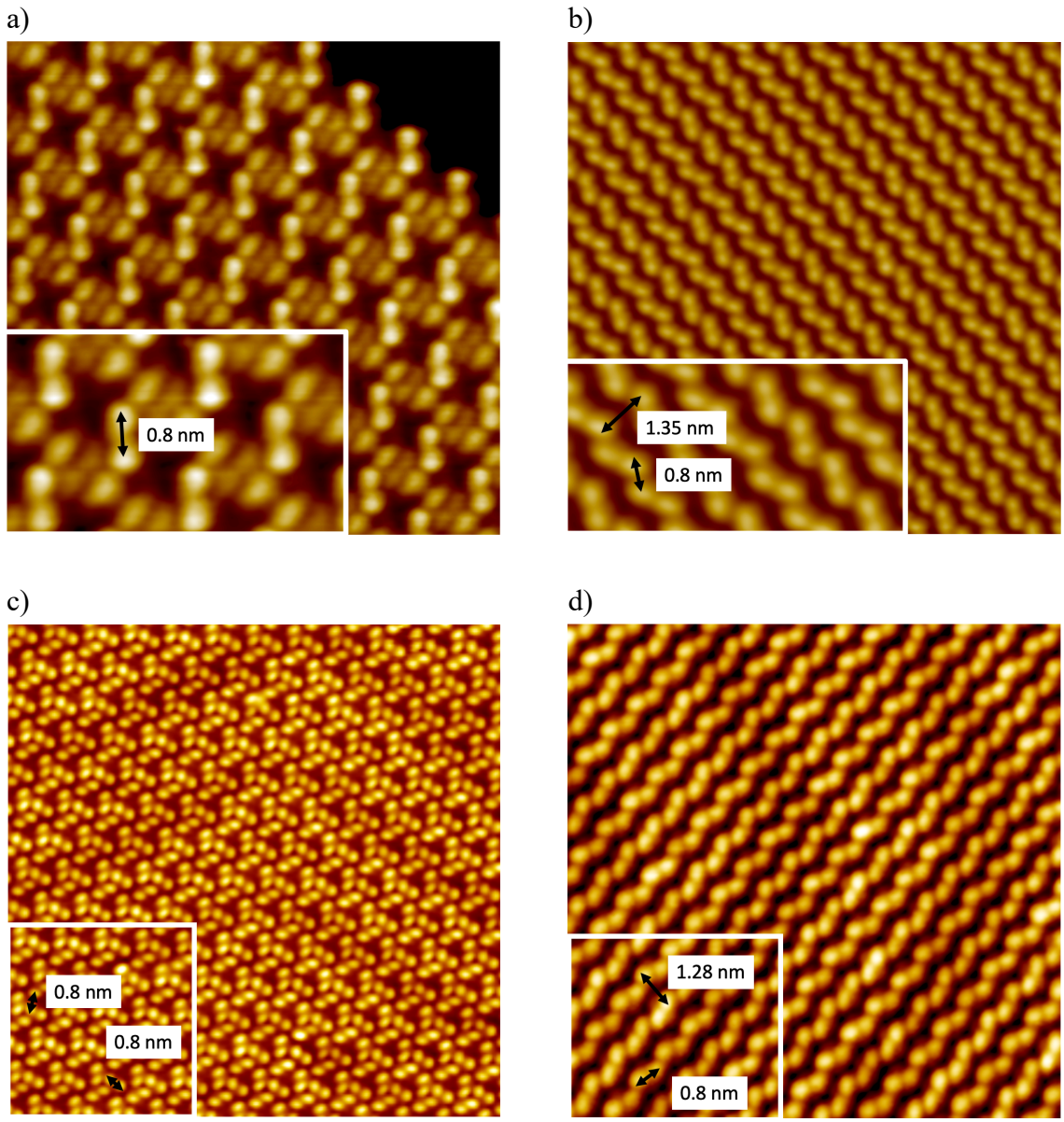

Figure 2. STM images of self-assembled molecules. a) PBA/Cu(111) (V_s = 0.9 V, I_t = 10 pA, 15 nm x 15 nm, inset 7 nm x 4 nm), b) CPBA/Cu(111) (V_s = -2.2 V, I_t = 10 pA, 20 nm x 20 nm, inset 8 nm x 4 nm), c) PBA/Au(111) (V_s = -1.5 V, I_t = 10 pA, 30 nm x 30 nm, inset 4 nm x 4 nm), d) CPBA/Au(111) (V_s = 1.5 V, I_t = 10 pA, 20 nm x 20 nm, inset 4 nm x 3 nm).

In the case of PBA/Cu(111) and CPBA/Cu(111) interfaces, large extended 2D islands are constituted by the periodic arrangement of several bright protrusions. The repeat unit pattern of each STM image is in accordance with the distance (0.8 ± 0.02 nm) between the edges of the topmost carbon ring of each of the two anthracenyl subunits of molecules (Figure 1). For PBA/Cu(111) interface, the repeat unit pattern is constituted by three pairs of disjoined protrusions rotated by 120° with different brightness (Figure 2a). In the case of CPBA/Cu(111) interface, 2D islands are made of bright lines separated by darker stripes. The periodicity between the bright lines is 1.35 ± 0.02 nm. Each line exhibits paired bright protrusions

separated by 0.8 ± 0.02 nm. In the case of PBA/Au(111) interface, the repetitive unit consists of three pairs of disjoined protrusions (Figure 2a) rotated by 120°. In each domain, all repetitive units are rotated only clockwise or only anti-clockwise, leading to homochiral domains. The distance measured between the disjoined protrusions is 0.8 ± 0.02 nm. For the CPBA molecules deposited on Au(111), a compact periodic network constituted by bright lines, which were separated by darker strips can be observed. The periodicity between the bright lines is 1.28 ± 0.02 nm. Each line is made up of paired bright protrusions separated by 0.8 ± 0.02 nm.

Based on our STM observations and measurements, we propose the models of the four investigated interfaces. On the basis of the features of PBA and CPBA molecules (Figure 1), each bright-paired protrusion observed in Figure 2 is attributed to a single PBA or CPBA molecule, respectively.

a)

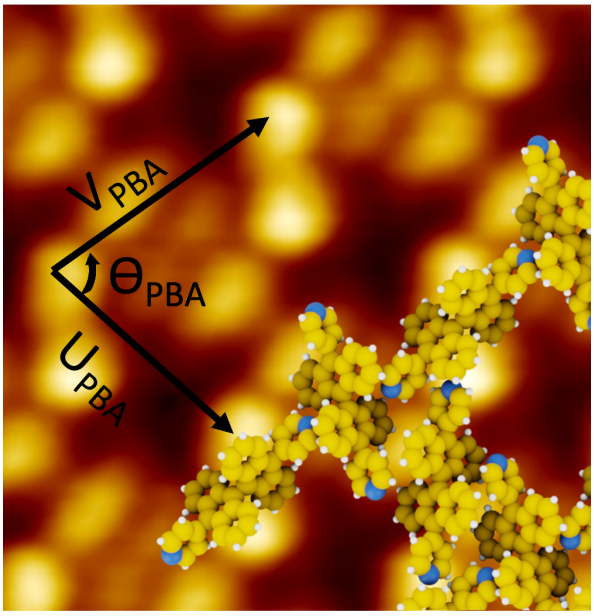

b)

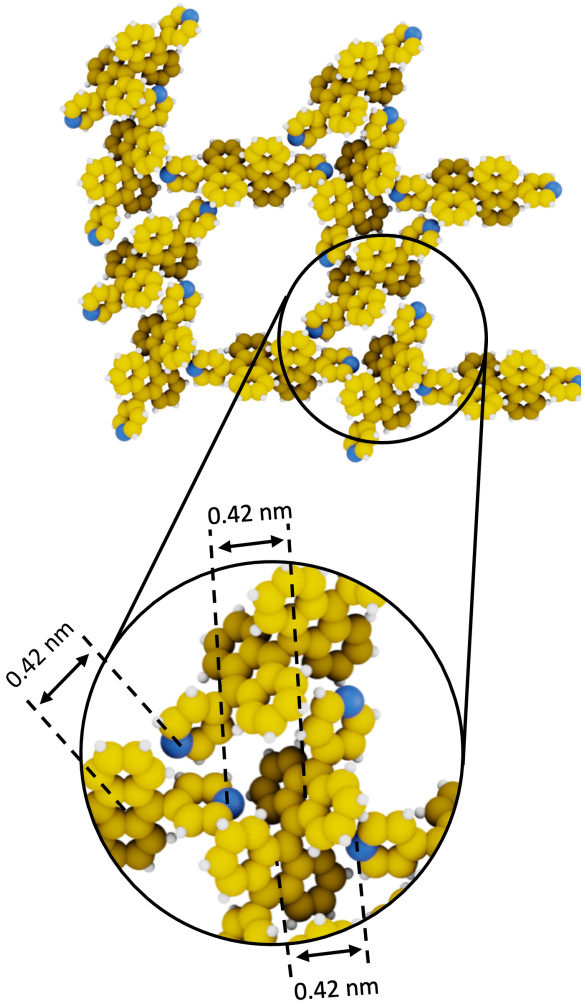

c)

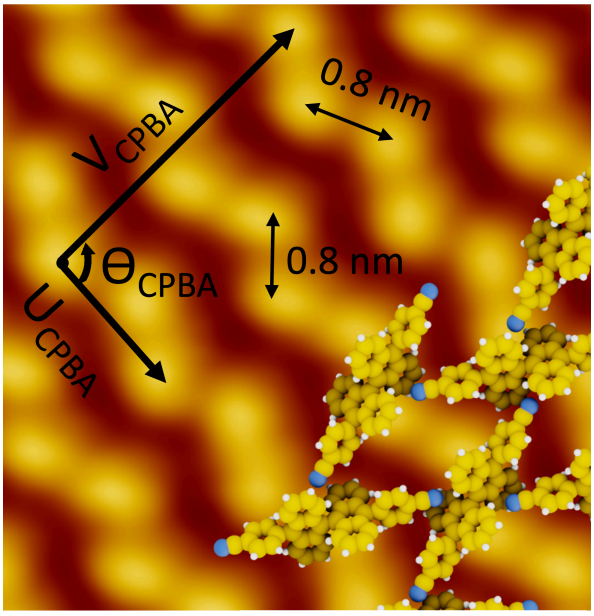
0.8 nm
V_{CPBA}
Θ_{CPBA}
0.8 nm
U_{CPBA}

d)

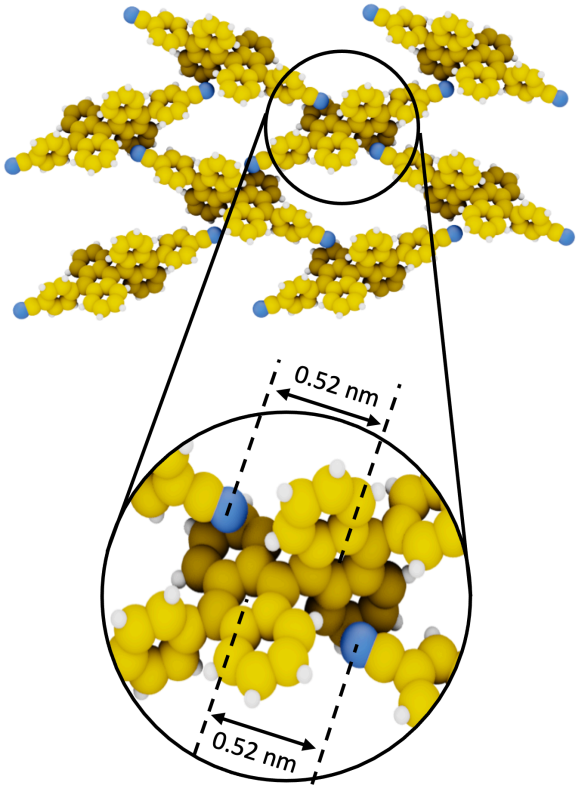
0.52 nm
0.52 nm

e)

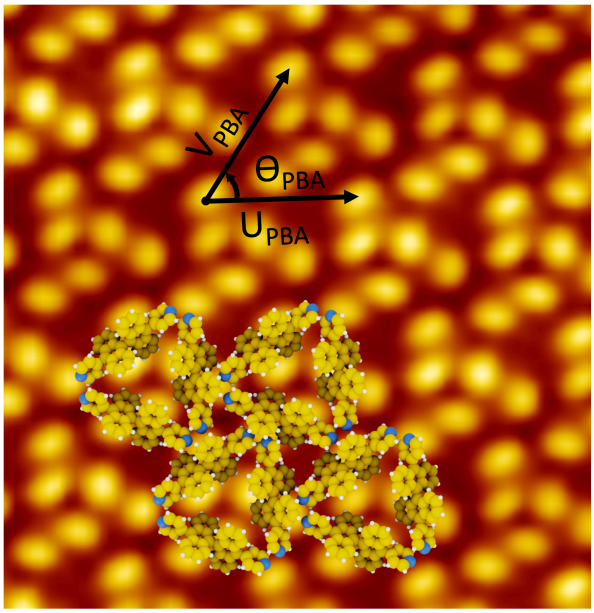
V_{PBA}
Θ_{PBA}
U_{PBA}

f)

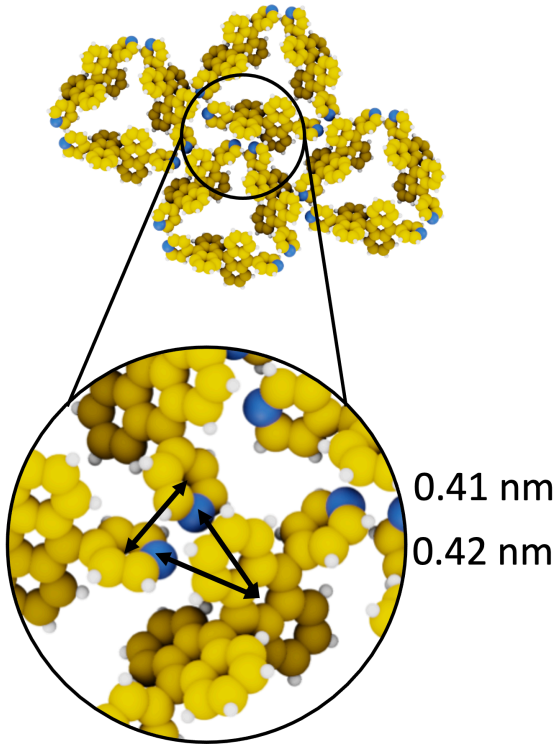
0.41 nm
0.42 nm

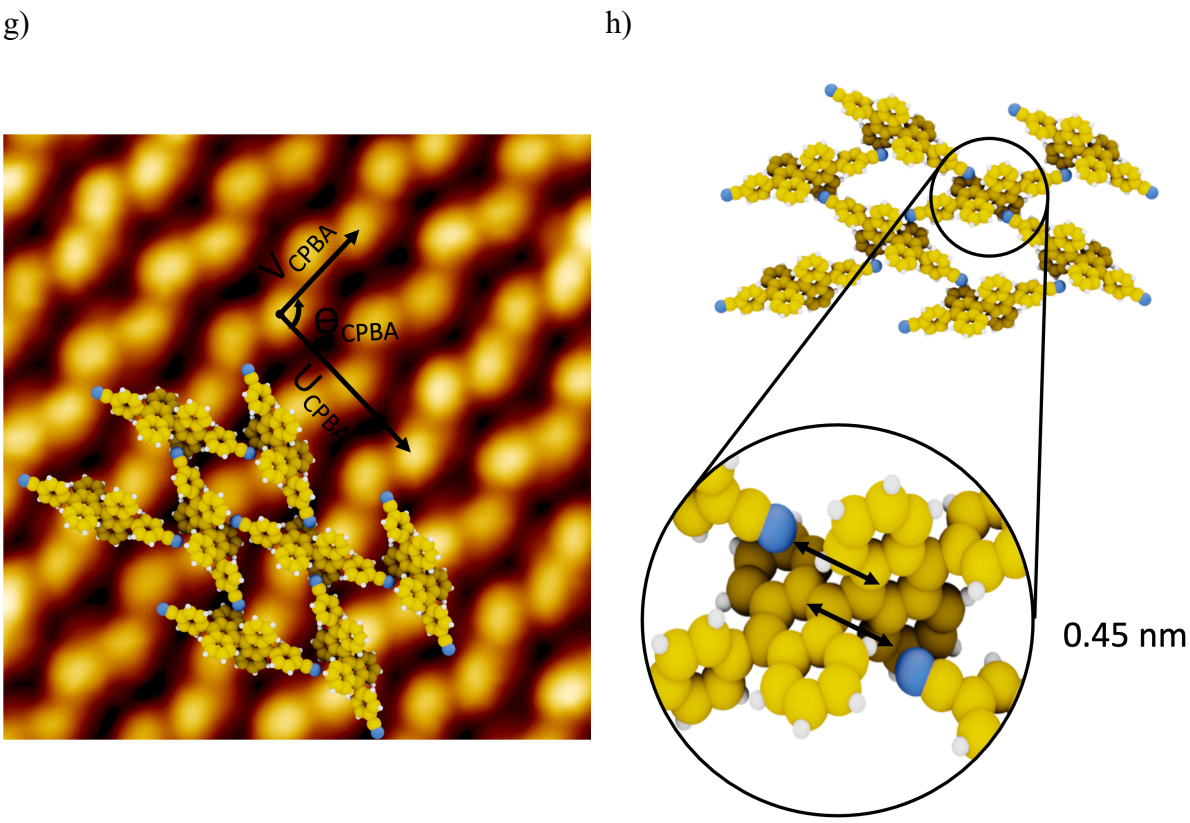

Figure 3. a) STM image of PBA supramolecular network on a Cu(111) surface with corresponding superimposed model and unit cell vectors: U_{PBA} = 1.98 nm, V_{PBA} = 2.20 nm, Θ_{PBA} = 77°, b) Representation of T-Shape π-π molecule-molecule interactions between adjacent pyridyl rings and the centre of the anthracenyl ring, separated by a distance of 0.42 nm, c) STM image of CPBA supramolecular network on a Cu(111) surface with corresponding superimposed model and unit cell vectors: U_{PBA} = 0.85 nm, V_{PBA} = 1.63 nm, Θ_{PBA} = 82°, d) Representation of T-Shape π-π molecule-molecule interactions between cyano-phenyl rings, pointing towards the centre of the anthracenyl ring (0.52 nm), e) STM image of PBA supramolecular network on an Au(111) surface with corresponding superimposed model and unit cell vectors: U_{PBA} = 2.25 nm, V_{PBA} = 2.25 nm, Θ_{PBA} = 60°, f) Representation of T-Shape π-π molecule-molecule interactions between two adjacent pyridyl rings, separated by a distance of 0.42 nm, and two nitrogen atoms point towards the centre of the anthracenyl ring of a third PBA molecule (0.41 nm), g) STM image of CPBA supramolecular network on an Au(111) surface with corresponding superimposed model and unit cell vectors: U_{CPBA} = 2.58 nm, V_{CPBA} = 1.45 nm, Θ_{CPBA} = 94°, h) Representation of T-Shape π-π molecule-molecule interactions between cyano moieties and the centre of the anthracenyl ring (0.45 nm).

The four investigated supramolecular networks are based on T-Shape π-π molecule-molecule interactions located between the lateral functional group (e.g. Pyridyl and cyano for PBA and CPBA, respectively, Figure 3) and the centre of the anthracenyl ring [42].

We investigated the chemical transformation of the four supramolecular self-assemblies induced by thermal annealing. Each supramolecular network was exposed to subsequent thermal annealing up to 673 K on both Cu(111) and Au(111) surfaces, respectively, from 1 hour to 4 hours. Below these two temperatures, all the starting self-assemblies are kept without any visible modification of the corresponding STM images.

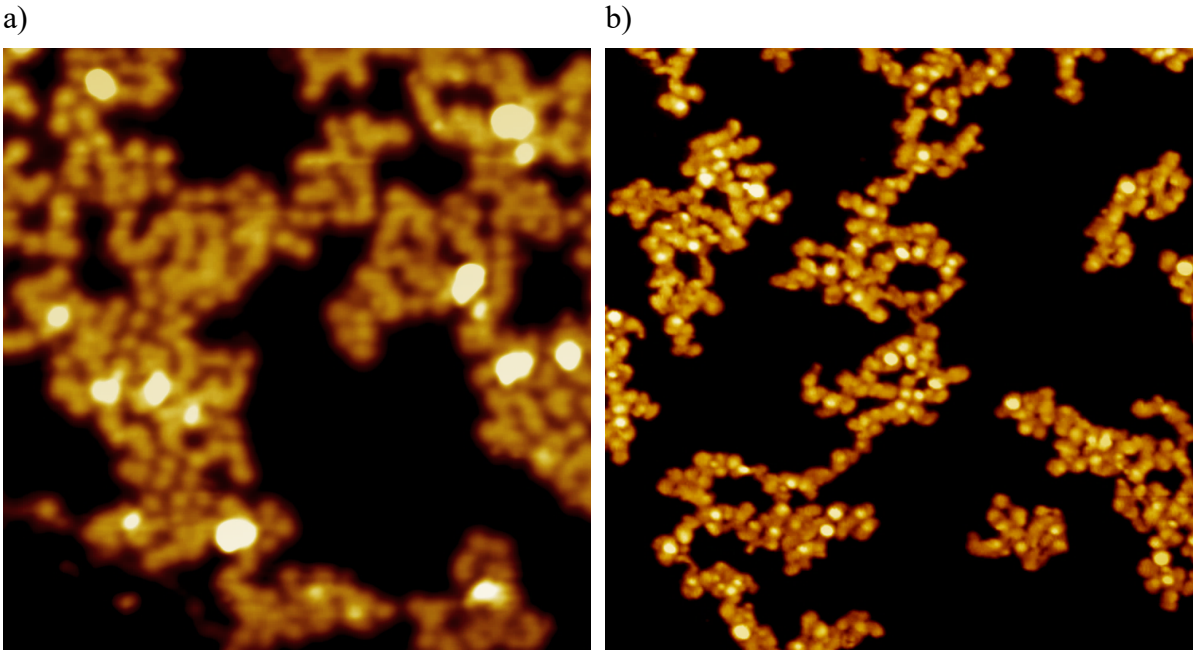

Figure 4. a) STM images of disordered features attained following subsequent thermal annealing up to 673 K on Cu(111) surface of : a) PBA (V_s = 1.8 V, I_t = 10 pA, 60 nm x 60 nm) an b) CPBA (V_s = -1.2 V, I_t = 10 pA, 60 nm x 60 nm).

On a Cu(111) surface, all observed post-annealing formed nanostructures are completely disordered (Figure 4), whatever is the duration or the temperature of annealing in the range of the previously described experimental procedure (e.g. 673-773 K, 1 to 4 hours, respectively). For temperatures above 773 K, only desorption phenomena was observed by decreasing the amounts of visible adsorbates inspected in corresponding STM images.

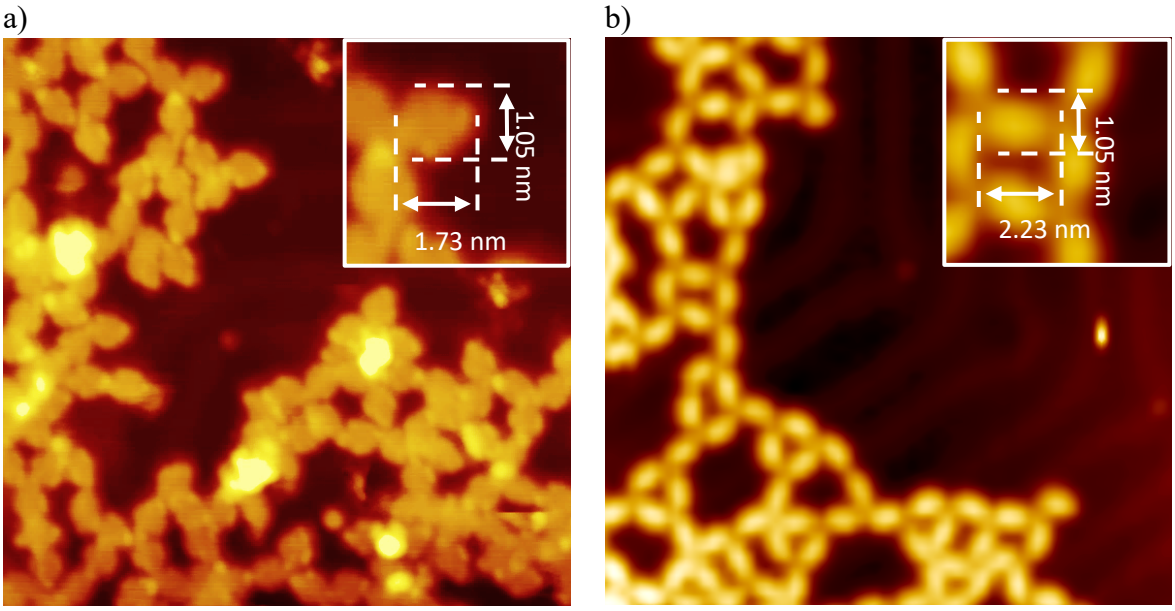

Figure 5. a) STM images of formed nanostructures on Au(111) surface upon thermal annealing at 673 K during one hour of : a) PBA (V_s = -2.8 V, I_t = 5 pA, 30 nm x 30 nm) an b) CPBA (V_s = -2.8 V, I_t = 5 pA, 30 nm x 30 nm). The width of each obtained nanostructures is 1.05 nm (see inset in the two STM images).

On a Au(111) surface, after thermal annealing, the two starting periodic supramolecular networks (Figure 2c-d) are transformed into disordered nanostructures (Figure 5). In addition, the resulting nanostructures are constituted by cross-shaped bright protrusions instead of bright-paired protrusions, as initially depicted in Figure 2c-d. The length of these new protrusions is 1.73 ± 0.05 nm and 2.23 ± 0.05 nm for PBA and CPBA, respectively while their width is 1.05 ± 0.05 nm. The bright protrusions lead to the formation of straight or reticulated nanolines including three- of four connecting nodes. The distance separating bright protrusions is longer in the case of CPBA than in the case of PBA (Figure 5).

Discussion

We made different thermal annealing, with temperatures from 400 K to 773 K. However, we never observed linear nanostructures corresponding to functionalized (3,1) GNRs, but only disordered features. This result is very surprising because, according to the reported reaction mechanism, the presence of aryl substituents at the 10 and 10' positions of a bianthryl building blocks should be in agreement with the formation of corresponding (3,1) GNRs [21-38]. However, as no (3,1) GNR was observed by using PBA and CPBA as building blocks on Au(111) and Cu(111) surfaces, we conclude that the surface-induced cleavage of C-H bond of 2 and 2' positions is not possible by annealing on a Cu(111). This claim is supported by the canonical forms of bianthryl molecule that govern the reactivity of fused six-membered aromatic rings. We assume that the thermally-induced cleavage of C-H bonds is only possible

on 10 and 10' positions on Cu(111) and Au(111) surfaces, to give biradical species that undergo to (3,1) GNRs [41]. In the case of PBA and CPBA molecules, as the 10 and 10' positions are substituted by pyridyl or cyanophenyl groups, respectively, the formation of (3,1) GNRs are impossible on the two investigated surfaces.

In the case of Cu(111) surface, which is a more reactive surface than Au(111) [43], the thermal annealing is strong enough to induce at least one C-H bond cleavage per PBA or CPBA molecules, but without any regiospecificity. Therefore, the resulting radicals, due to surface-assisted C-H bond cleavages, lead to the formation of disordered nanostructures (Figure 6), as observed on STM images (Figure 4).

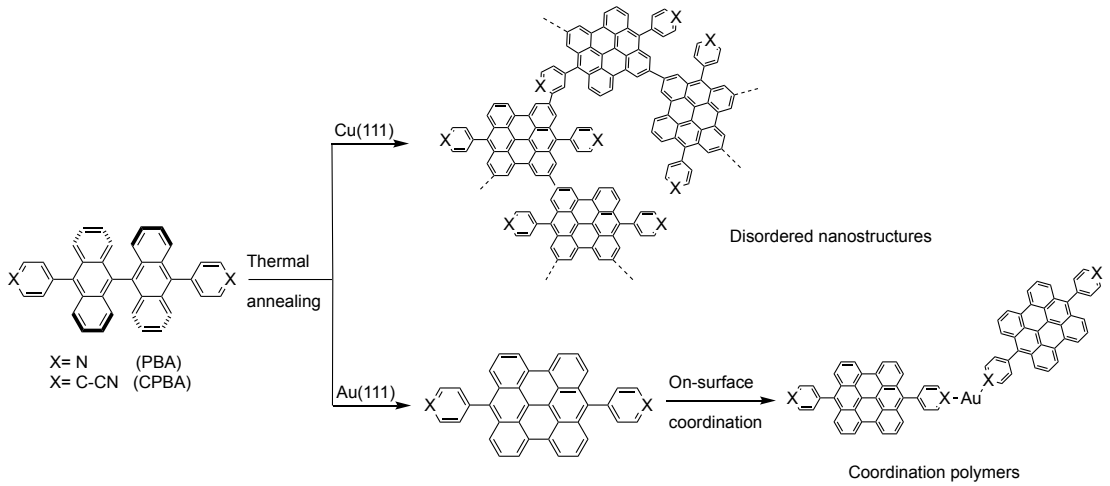

Figure 6. Thermal-induced transformation of PBA and CPBA molecules on a Cu(111) and an Au(111) surface. On Cu(111), the thermal annealing leads to disordered nanostructures, while on Au(111) the starting molecules are flattened due to intramolecular cyclodehydrogenation reactions.

In the case of Au(111) surface, the cleavage of C-H bonds to lead to radicals is not possible. However, thermal annealing can induce intramolecular cyclodehydrogenation reactions. This type of reaction is well-known on Au(111) surface [21-28]. The driven force of cyclodehydrogenation is the formation of more conjugated compounds. One consequence of this increased conjugation is the flattening of involved molecules. By the way, the average distance between Au(111) surface and flat-PBA or flat-CPBA molecules is shorter than those between surface and respectively, PBA and CPBA (Figure 6). Therefore, the interaction of nitrogen atoms of pyridyl or cyanophenyl moieties with the gold atoms of the surface is reinforced, which promotes the formation of coordination polymers [44-46]. The pyridyl or cyano moieties are ligand for several kind of metal atoms, due to the presence of the lone pair of electrons on the nitrogen atom. Due to the strength and the directionality of these metal-ligand bonds, the corresponding coordination polymers exhibit a high degree of reticulation on metal substrates like on an Au(111) surface, even if it is still rare compared to other coinage surfaces [44-46]. These coordination properties support the observation of straight and reticulated nanolines in STM images (Figure 5).

Conclusions

We have investigated the on-surface chemistry of two 10,10'-disubstituted-9,9'-bianthryl derivatives induced by a thermal annealing on Cu(111) and Au(111) surfaces. We have demonstrated that the choice of building blocks strongly alters the on-surface chemical behavior The presence of aryl substituents on the 10,10'-poisitions avoid the formation of mandatory radicals which are implied in the formation of (3,1)-GNRs. Depending of the reactivity of the surface, we have shown that 2D-extended periodic supramolecular networks are converted into coordination polymers on Au(111) surface while they led to highly disordered nanostructures on the Cu(111) surface. This strategy paves the way to new possibilities for multi-functional nanostructures by using on-surface assisted synthesis.

Acknowledgments

The authors acknowledge the financial support from the French National Research Agency through contract OVATION (ANR-19-CE09-0020) and from the Pays de Montbéliard Agglomération. The authors thank Pr. Dr. Alain Rochefort (Polytechnique Montréal, Canada) for fruitful discussions.

References

1. L. Xing, Z. Peng, W. Li and K. Wu, *Acc. Chem. Res.,* **52**, 1048 (2019).
2. J. V. Barth, G. Costantini, K. Kern, *Nature*, **437**, 671 (2005).
3. T. Kudernac, S. Lei, J. A. A. A. W. Elemans and S. De Feyter, *Chem. Soc. Rev.*, **38**, 402 (2009).
4. L. Sosa-Vargas, E. Kim and A.-J. Attias, *Mater. Horiz.*, **4**, 570 (2017)
5. Y. Makoudi, J. Jeannoutot, F. Palmino, F. Chérioux, G. Copie, C. Krzeminski, F. Cléri and B. Grandidier, *Surf. Sci. Report*, **72**, 316 (2017).
6. L. Grill, M. Dyer, L. Lafferentz, M. V. Persson and S. Hecht, *Nat. Nanotech.*, **2**, 687 (2007).
7. M. Matena, T. Riehm, M. Stöhr, T. A. Jung and L. H. Gade, *Angew. Chem. Int. Ed.*, **47**, 2414 (2008).
8. F. Palmino, C. Loppacher and F. Chérioux, *ChemPhysChem*, **20**, 2271 (2019).
9. P. A. Held, H. Fuchs and A. Studer, *Chem. Eur. J.,* **23**, 5874 (2017).
10. B. Yang, B. Dong and L. Chi, *ACS Nano*, **14**, 6376 (2020).
11. S. Clair and D. G. de Oteyza, *Chem. Rev.*, **119**, 4717 (2019).
12. M. Lackinger, *Polym. Inter.*, **64**, 1073 (2015).
13. N. Pvalicek, Z. Majzik, S. Collazos, G. Meyer, D. Perez, E. Guitian, D. Pena and L. Gross, *ACS Nano*, **11**, 10768 (2017).
14. F. Para, F. Bocquet, L. Nony, C. Loppacher, M. Féron, F. Chérioux, D. Z. Gao, F. F. Canova and M. B. Watkins, *Nature Chem.*, **10**, 1112 (2018).
15. S. Kawai, H. Sang, L. Kantorovitch, K. Takahashi, K. Nozaki and S. Ito, *Angew. Chem., Int. Ed.*, **59**,10842 (2020).
16. E. Geagea, J. Jeannoutot, M. Féron, F. Palmino, C. M. Thomas, A. Rochefort and F. Chérioux, *Nanoscale*, **13**, 349 (2021).
17. L. Grossmann, B. T. King, S. Reichlmaier, N. Hartmann, J. Rosen, W. M. Heckl, J. Bjork and M. Lackinger, *Nature Chem.*, **13**, 730 (2021).
18. L. Grill, S. Hecht, *Nature Chem.* **12**, 115 (2020).
19. D. J. Rizzo, G. Veber, T. Cao, C. Bronner, T. Chen, F. Zhao, H. Rodriguez, S. G. Louie, M. F. Crommie and F. R. Fischer, *Nature*, **560**, 204 (2018).
20. O. Gröning, S. Wang, X. Yao, C. A. Pignedoli, G. Borin Barin, C. Daniels, A. Cupo, V. Meunier, X. Feng, A. Narita, K. Mullen, P. Ruffieux and R. Fasel, *Nature*, **560**, 209 (2018).

21. L. Cai, P. Ruffieux, R. Jaafar, M. Bieri, T. Braun, M. Blankenburg, A. P. Seitsonen, M. Saleh, X. Feng, K. Mullen and R. Fasel, *Nature* **2010**, *466*, 470 (2010).
22. H. Sakaguchi, S. Song, T. Kojima and T. Nakae, Homochiral Polymerization-Driven Selective Growth of Graphene Nanoribbons. *Nature Chem.*, **9**, 57 (2017).
23. D. G. de Oteyza, A. Garcia-Lekue, M. Vilas-Varela, N. Merino-Diez, E. Carbonell-Sanroma, M. Corso, G. Vasseur, C. Rogero, E. Guitan, J. I. Pascual, J. E. Ortega, Y. Wakayama and D. Pena, *ACS Nano,* **10**, 9000 (2016).
24. P. Ruffieux, S. Wang, B. Yang; C. Sanchez-Sanchez, J. Liu, T. Dienel, L. Tarliz, P. Shinde, C. A. Pignedoli, D. Passerone, T. Dumslaff, X. Feng, K. Mullen and R. Fasel, *Natur*e, **531**, 489 (2016).
25. J. Cai, C. A. Pignedoli, L. Talirz, P. Ruffieux, H. Söde, L. Liang, V. Meunier, R. Berger, R. Li, X. Feng, K. Mullen and R. Fasel, *Nature Nano.,* **9**, 896 (2015).
26. P. Ruffieux, J. Cai, N. C. Plumb, L. Pathey, D. Prezzi, A. Ferretti, E. Molinari, X. Feng, K. Mullen, C. A. Pignedoli and R. Fasel, *ACS Nano*, **6**, 6930 (2012).
27. C. Moreno, M. Vilas-Varela, B. Kretz, A. Garcia-Lekue, M. Costache, M. Paradinas, M. Panighel, G. Ceballos, S. O. Valenzuela, D. Pena and A. Mugarza, *Science*, **360**, 199 (2018).
28. S. Kawai, S. Nakatsuka, T. Hatakeyama, R. Pawlak, T. Meier, J. Tracey, E. Meyer and A. S. Foster, *Sci. Advances*, **4**, eaar7181 (2018).
29. Z. Chen, H. I. Wang, N. Bilbao, J. Teyssandier, T. Prechtl, N. Cavani, A. Tries, R. Biagi, V. de Renzi, X. Feng, M. Klau, S. De Feyter, M. Bonn, A. Narita and K. Mullen, *J. Am. Chem. Soc.*, **139**, 9483 (2017).
30. Z. Chen, A. Narita and K. Mullen, *Adv. Mater.,* **32**, 2001893 (2020).
31. L. Tarliz, P. Ruffieux and R. Fasel, *Adv. Mater.,* **28**, 6222 (2016).
32. C. Sanchez-Sanchez, T. Dienel, O. Deniz, P. Ruffieux, R. Berger, X. Feng, K. Mullen and R. Fasel, *ACS Nano*, **10**, 8006 (2016).
33. P. Han, K. Akagi, F. Federici Canova, R. Shimizu, H. Oguchi, S. Shiraki, P. S. Weiss, N. Asao and T. Hitosugi, *ACS Nano*, **9**, 12035 (2015).
34. K. A. Simonov, N. A. Vinogradov, A. S. Vinogradov, A. V. Generalov, E. M. Zagrebina, N. Mårtensson, A. A. Cafolla, T. Carpy, J. P. Cunniffe and A. B. Preobrajenski, *J. Phys. Chem. C*, **118**, 12532 (2014).
35. F. Schulz, P. H. Jacobse, F. F. Canova, J. van der Lit, D. Z. Gao, A. von den Hoogenband, P. Han, R. J. M. Kelin Gebbink, M.-E. Moret, P. M. Joensuu, I. Swart and P. Liljeroth, *J. Phys. Chem. C*, **121**, 2896 (2017).
36. P. Han, K. Akagi, F. F. Canova, H. Mutoh, S. Shiraki, K. Iwaya, P. Weiss, N. Asao and T. Hitosugi, *ACS Nano*, **8**, 9181 (2014).
37. K. A. A Simonov, N. A. Vinogradov, S. A. Vinogradov, A. V. Generalov, E. M. Zagrebina, N. Martensson, A. A. Cafolla, T. Carpy, J. P. Cunniffe and A. B. Preobrajenski, *ACS Nano*, **9**, 3399 (2015).
38. P. Han, K. Akagi, F. F. Canova, H. Mutoh, S. Shiraki, K. Iwaya, P. Weiss, N. Asao and T. Hitosugi, *ACS Nano*, **9**, 3404 (2015).
39. P. Natarajan and M. J. Schmittel, *J. Org. Chem.*, **78**, 10383 (2013).
40. N. Miyaura and A. Suzuki, *Chem. Rev.*, **95**, 2457 (1995).
41. E. Geagea, J. Jeannoutot, L. Morgenthaler, S. Lamare, A. Rochefort, F. Palmino and F. Chérioux, *Chem. Commun.*, **57**, 6043 (2021).
42. C. R. Martinez and B. L. Iverson, *Chem. Sci.*, **3**, 2191 (2012).
43. S. Duhm, A. Gerlach, I. Salzmann, B. Broker, R. L. Johnson, F. Schreiber and N. Koch, *Org. Elec.*, **9**, 111 (2008).
44. L. Dong, Z. Gao and N. Lin. *Prog. Surf. Sci.*, **91**, 101 (2016).
45. M. Koepf, F. Chérioux, J. A. Wytko and J. Weiss. *Coord. Chem. Rev.*, **256**, 2872 (2012).
46. Q. Fan, C. Wang, Y. Han, J. Zhu, J. Kuttner, G. Hilt and J. M. Gottfried. *ACS Nano*, **8**, 709 (2014).